Sustainable lignin nanofiber electrodes for vanadium redox flow batteries

Emihle Tyandela[1], *Nkosikho* Dlangamandla[2], *Tendai* Tawonezvi[3], and *Myalelo* Nomnqa*[4]

[1]Department of Chemical Engineering, Faculty of Engineering and the Built Environment, Cape Peninsula University of Technology, Symphony Way, Bellville, Cape Town, 7535, South Africa.
[2]Department of Civil Engineering, Faculty of Engineering and the Built Environment, Cape Peninsula University of Technology, Symphony Way, Bellville, Cape Town, 7535, South Africa.
[3]South African Institute of Advanced Materials Chemistry, Faculty of Natural Science, University of the Western Cape, Robert Sobukwe, Bellville, Cape Town, 7535, South Africa.
[4]Department of Chemical Engineering Technology, Faculty of Engineering and the Built Environment, University of Johannesburg, P.O Box 17011, Doornfontein, Johannesburg 2088, South Africa.

Abstract: The development of sustainable, high-performance electrode materials is a challenge in advancing vanadium redox flow battery (VRFB) technology for large-scale electrochemical energy storage. This study investigates the fabrication of lignin-based carbon nanofibers (LCNFs) via electrospinning as a renewable and cost-effective alternative to conventional PAN-based carbon electrodes. Alkali lignin blended with polyvinylpyrrolidone PVP in a 1:1 mass ratio was dissolved in N, N-dimethylformamide (DMF) at total polymer concentrations of 15, 17.5, 20, and 21.70 wt%, and electrospun under systematically varied process conditions using a central composite design (CCD) framework. Scanning electrode microscopy (SEM) characterisation revealed a clear concentration-dependent evolution in fiber morphology: beaded, discontinuous fibers at 15 wt% transitioned to well-developed, bead-free, interconnected nanofiber networks at 20 wt% and above, with mean fiber diameters ranging from 163 nm to 476 nm. Thermal stabilisation in air at 250°C and subsequent carbonisation under nitrogen at 600°C preserved the fibrous structure while imparting electrical conductivity to the mats. Electrochemical characterisation by cyclic voltammetry in a 0.05 M vanadium electrolyte showed a quasi-rectangular profile indicative of a mixed capacitive-faradaic charge storage mechanism. The LCNF electrode exhibited stable current response scaling with scan rate from 10 to 500 mV/s, with current density increasing from ±0.5 mA/g to ±6 mA/g, confirming good rate capability and reversible charge storage behaviour.

1 Introduction

The accelerating global transition toward renewable energy sources has placed unprecedented demand on large-scale, long-duration electrochemical energy storage technologies. Redox flow batteries (RFBs) are becoming the preferred energy storage option for large-scale use because of their capacity to store substantial amounts of energy per unit of volume over long durations with scalable and flexible design. Among the various RFB systems, all VRFB has attracted immense research and commercial interest [1]. VRFBs are prominent in large-scale energy storage because of their long cycle life, high energy efficiency, and cost-effectiveness for storage capacities over hours. Furthermore, VRFBs present advantages, including zero cross-contamination, scalability, long life cycle and non-toxic operating conditions [2, 3]. Unlike lithium-ion batteries, VRFBs can easily increase their energy capacity by increasing the volume of the vanadium electrolyte, making them suitable for long-duration energy storage needs. Additionally, VRFBs provide cycle life greater than 10,000 cycles, are inherently safe due to their non-flammable liquid electrolyte and the vanadium electrolyte is recyclable [4].

Notwithstanding these features, the widespread adaptation of VRFBs remains limited by technical and economic challenges. Enhancing the power density of vanadium redox flow batteries is essential for reducing costs and improving efficiency, requiring comprehensive, collaborative optimisation of electrode materials. Conventional electrodes, typically carbon felt or graphite felt suffer from low electrochemical performance, such as poor conductivity, which hinders their commercial

*Corresponding author: myalelon@uj.ac.za

© The Authors, published by EDP Sciences. This is an open access article distributed under the terms of the Creative Commons Attribution License 4.0 (https://creativecommons.org/licenses/by/4.0/).

viability. In particular, the limited surface area, poor wettability, and sluggish reaction kinetics of these materials toward both the VO^{2+}/VO_2^+ and V^{2+}/V^{3+} redox couples have motivated an extensive search for an advanced electrode structure [5].

Electrospinning has thus emerged as a versatile and scalable technique for fabricating carbon nanofiber (CNF) electrodes for VRFBs. The enhanced surface area of electrospun mats made of nanofibers provides abundant active sites for redox reactions and can improve electron transfer compared to commercial carbon felt [6]. Nevertheless, the environmental and cost profile of the electrode fabrication process itself is increasingly scrutinised. Currently, polyacrylonitrile (PAN) which is derived from diminishing petroleum resources is the most common precursor used in production. electrospun carbon nanofibers. This underscores the urgency of developing alternative, bio-derived precursors that reduce both environmental burden and material cost.

Lignin is an exceptionally attractive candidate for this purpose. Lignin is the second most abundant source of renewable carbon, possessing an aromatic structure that makes it a strong candidate for carbon fiber production [7]. It is generated in large quantities as a byproduct of cellulose extraction in the bioethanol sector and the pulp and paper industry. From a materials perspective, lignin, the most abundant polyphenolic compound in nature, boasts a substantial number of aromatic backbones with up to 60% carbon content, making it an ideal potential precursor for carbon fibers [7]. The conversion of lignin into CNFs via electrospinning and subsequent carbonisation has been demonstrated across a range of energy storage applications. For VRFB electrodes specifically, lignin-derived electrospun carbon mats have exhibited higher activity toward the VO^{2+}/VO_2^+ reaction than commercial carbon papers, attributed to higher surface area and a greater abundance of oxygen functional groups at the surface [8-10]. Complementary research has demonstrated that carbon nanofibres produced by the electrospinning of lignin can be used as electrodes for vanadium electrochemistry, and their properties can be customised to enhance electrochemical performance by adjusting lignin type, electrospinning parameters, and thermal treatment conditions. [7, 8].

However, key challenges remain. The low molecular weight and irregular structure of lignin pose significant challenges for electrospinning, and achieving stable, high-performance CNFs typically requires blending lignin with carrier polymers. Moreover, the relationship between lignin source, fiber morphology, surface chemistry, and electrochemical performance in full VRFB cell configurations is not yet fully understood. In this work, we evaluate the influence of electrospinning operation conditions on fiber morphology, structural properties, and electrochemical activity toward both vanadium redox couples.

2 Materials and Methods

2.1 Materials

Alkali lignin (99%, Angene), polyvinylpyrrolidone (PVP; Mw = 1,300,000 g/mol by LS, 99%, Sigma-Aldrich), and N, N-dimethylformamide (DMF; Mw = 73.05 g/mol, 99.5%, Thermo-Scientific) were used as received without further purification. Vanadium commercial electrolyte solution (V(III)/V(IV)) of 1.57 M (Oxkem), with a sulphuric acid concentration of 4.19 M, and a phosphoric acid content of 0.1 M was also used.

2.2 Preparation of LCNFs

2.2.1 Spinning Solution Preparation

Lignin and PVP were dissolved in DMF at a 1:1 mass ratio under continuous magnetic stirring at room temperature for 24 hours. Three total polymer concentrations were prepared: 15, 17.5, and 20 wt%. The 1:1 ratio was selected to maximise lignin content while relying on the high-molecular-weight PVP to provide the chain entanglement necessary for stable fiber formation, as pure lignin alone lacks sufficient molecular weight to sustain a continuous electrospinning jet.

2.2.2 Electrospinning

Nanofibers were synthesised using a stationary needle-based electrospinning setup with a flat aluminium collector. A constant positive voltage of +18 kV and a negative voltage of -3 kV was applied to the needle and collector, respectively, and maintained unchanged throughout all experiments. The application of a negative voltage to the collector in addition to the positive voltage at the needle tip serves to strengthen the effective electric field driving the jet, thereby enhancing fiber deposition and promoting the formation of thinner, more uniform fibers. Three process parameters were varied to assess their influence on fiber morphology: total polymer concentration (15, 17.5, and 20 wt%), needle-to-collector distance (10, 12.5, and 15 cm), and volumetric flow rate (0.175, 0.200, and 0.225 mL/h), as summarised in Table 1. These parameters directly influence fiber diameter and morphology by controlling the degree of solvent

evaporation and the stability of the electrospinning jet prior to fiber deposition.

Table 1: Electrospinning parameters investigated in this study

Parameters	Level 1	Level 2	Level 3
Concentration (wt%)	15	17.5	20
Spinning Distance (cm)	10	12.5	15
Flow rate (mL/h)	0.175	0.2	0.25
Lignin: PVP ratio	1:1	-	-
Applied Voltage (kV)	+18/-3 (constant)	-	-

2.2.3 Stabilisation and Carbonisation

As-spun fiber mats were thermally stabilised in air at 250 °C (at a heating rate of 1 °C min^{-1}) to promote crosslinking and prevent fiber fusion during subsequent carbonisation. This oxidative step converts the thermoplastic lignin precursor into a thermoset-like structure capable of retaining fiber geometry at high temperatures. Carbonisation was then carried out under flowing nitrogen at high temperature, following a slow initial ramp of 5 °C min^{-1} to 600 °C final target temperature, after which the mats were cooled under nitrogen to room temperature. Carbonisation under an inert atmosphere converts the stabilised organic precursor into electrically conductive carbon nanofibers through progressive elimination of non-carbon elements. The best-performing carbonised sample was subsequently selected for characterisation.

2.3 Characterisation

2.3.1 Structural Morphology

The morphology of as-spun, pre-oxidised, and carbonised lignin-based carbon nanofiber (LCNF) was examined using scanning electron microscopy (SEM, Jeol JCM700)

2.3.2 Electrochemical characterisation

The electrochemical performance of the best-performing carbonised lignin-based nanofiber electrode was assessed by cyclic voltammetry (CV) using a three-electrode cell configuration, comprising an RDE packed with the electrospun carbon nanofibers as the working electrode, a graphite plate as the counter electrode, and an Ag/AgCl reference electrode. The electrolyte was prepared by diluting a 1.6 M vanadium stock solution to a final concentration of 0.05 M. Dilute vanadium solutions are preferred in three-electrode CV studies as they reduce mass-transport limitations, ensuring the measured response reflects the intrinsic kinetics of the electrode surface.

The cell was maintained under a continuous nitrogen purge throughout all measurements. This is particularly important for the V^{2+}/V^{3+} couple, as atmospheric oxygen can introduce inaccurate oxidation signals that distort the electrochemical response. All electrodes were connected to a Metrohm Autolab potentiostat operated via Nova software. CV scans were performed between 10-500 mV/s over a potential window of -0.71 V to 0.39 V vs. Ag/AgCl.

3 Results and Discussion

3.1 Fiber morphology and evaluation

The electrospinning process parameters investigated in this study, including solution concentration, flow rate, and collector distance, were systematically varied according to a central composite design (CCD) generated using Design Expert software. The slight variations observed in certain parameter values, such as the 21.70 wt% concentration and the 0.242 ml/h flow rate, are a direct consequence of the alpha (α) factor inherent to the CCD framework, which defines the axial points of the design space and necessarily introduces values that extend marginally beyond the factorial boundaries of the experimental domain. It is important to note, however, that during electrospinning, at tip to collector distances of 10 cm and below no fiber deposition was found to occur regardless of the polymer concentration employed, as the insufficient flight distance between the needle tip and the collector prevented adequate solvent evaporation and fiber solidification, resulting in electrospraying rather than solid nanofibers.

The SEM micrographs demonstrate a clear concentration-dependent evolution in fiber morphology across the three lignin solution concentrations investigated, as shown in Figure 1. At 15 wt% demonstrated in Figure 1 (A and B), the electrospun fibers exhibit a predominantly beaded morphology, characterised by numerous large, spherical beads distributed along thin, discontinuous fiber segments in a classic beads-on-a-string arrangement. Both samples were electrospun at a fixed collector distance of 15 cm, but at different flow rates of 0.175 and 0.225 ml/h, yielding mean fiber diameters of 163 nm and 196 nm, respectively. The observed increase in fiber diameter with increasing flow rate at this concentration is consistent with a high

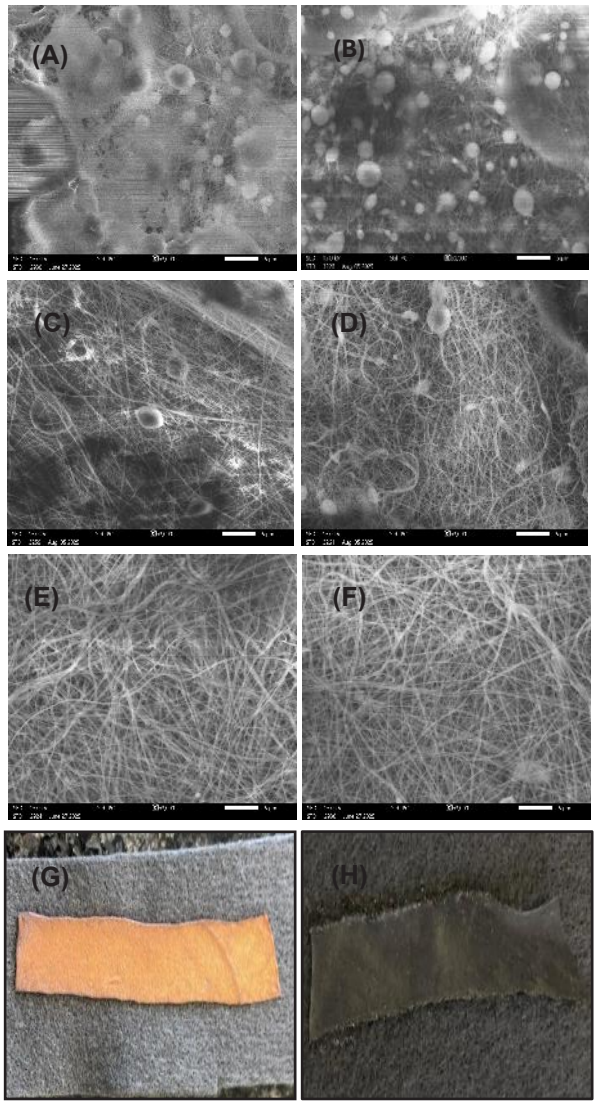

Fig 1. As-spun nanofibers formed by electrospinning from a 15 wt% solution at a spinning distance of 15 cm: A & B) As-spun and Stabilised at a flow rate of 0.175 ml/h, C&D) As-spun and Stabilised at a flow rate of 0.225 ml/h, respectively.

volumetric polymer supply to the electrospinning jet, though the solution remained insufficiently viscous to suppress bead formation. This defective morphology is attributable to insufficient polymer chain entanglement at this lower concentration, which destabilises the electrospinning jet and promotes surface tension-driven bead formation rather than continuous fiber elongation.As the concentration is increased to 17.5 wt% as shown in Figure 1 (C) and (D), a transitional morphology becomes apparent, wherein bead density is markedly reduced, and fibers become increasingly continuous and more uniform in diameter, reflecting improved viscoelastic properties of the spinning solution that partially suppress bead formation. These samples were electrospun at a collector distance of 12.5 cm and flow rates of 0.242 and 0.200 ml/h, producing fiber diameters of 220 nm and 219 nm, respectively. The remarkably similar fiber diameters obtained at this concentration despite the differing flow rates suggest that at 17.5 wt%, the solution viscosity plays a more dominant role in governing fiber diameter than flow rate alone, and that the system is approaching a rheological threshold conducive to stable jet formation.

At the highest concentration investigated, which was 20 wt% as shown in Figure 1 (E) and (F), a well-developed, bead-free nanofiber network is observed, consisting of dense, continuous, and randomly oriented fibers with a high degree of diameter uniformity. These fibers were also electrospun at a collector distance of 15 cm, at flow rates of 0.175 and 0.225 ml/h, yielding fiber diameters of 264 nm and 270 nm, respectively. The progressive increase in mean fiber diameter from 163-196 nm at 15 wt% to 264-270 nm at 20 wt% across comparable processing conditions underscores the dominant influence of solution concentration and viscosity on fiber formation, as higher entanglement density restricts jet thinning during whipping and elongation. This morphology indicates that sufficient chain entanglement and solution viscosity were achieved at this concentration to stabilise the Taylor cone and produce a consistent electrospinning jet, yielding an interconnected porous mat structure ideal for subsequent thermal processing.

Following electrospinning, the fiber mats were subjected to stabilisation and carbonisation, the outcomes of which are captured in Figure 1 (G) and (H), respectively. The stabilised mat in Figure 1 (G) displays a distinctive orange-brown colour, which is characteristic of lignin-based fibers that have undergone oxidative thermal stabilisation, typically carried out in air at 250°C. At this stage, the mat retains its structural integrity, appearing dimensionally stable and uniform. In contrast, the carbonised mat in Figure 1 (H) exhibits a deep black appearance consistent with the conversion of the organic precursor into a carbon-rich structure following pyrolysis under an inert atmosphere at 600°C. The mat undergoes shrinkage which are commonly associated with significant mass loss and thermal contraction during the carbonisation process. Importantly, however, the fibrous structure of the mat is largely preserved through carbonisation (as shown in Figure 2), confirming that the stabilisation step effectively prevented structural collapse, and demonstrating the potential of these lignin-based carbon nanofiber mats for applications in energy storage electrodes.

The electrospinning of a 21.70 wt% polymer solution with a flow rate of 0.200 mL/h produced continuous, bead-free nanofibers in the as-spun state, as shown in Figure 2 (A) of which all characterisations done in this paper will be based. The corresponding fiber diameter distribution

histogram in Figure 2 (B) shows an average diameter (AD) of 476.51 nm with a relatively narrow and approximately symmetrical distribution, with the majority of fibers falling within the 300-600 nm range. The complete absence of beads or beaded fibers is noteworthy and indicates that the selected electrospinning parameters were well within the stable jetting regime for this lignin system, despite the relatively high total polymer concentration. The well-entangled polymer chains at 21.70 wt% provided sufficient viscoelastic resistance to suppress surface tension-driven instabilities during jet elongation, yielding a morphologically uniform and interconnected nanofiber mat. This bead-free morphology is particularly advantageous for subsequent thermal processing, as structural defects such as beads can act as stress concentration points during shrinkage and may compromise the mechanical integrity and electrochemical performance of the final carbon nanofiber mat.

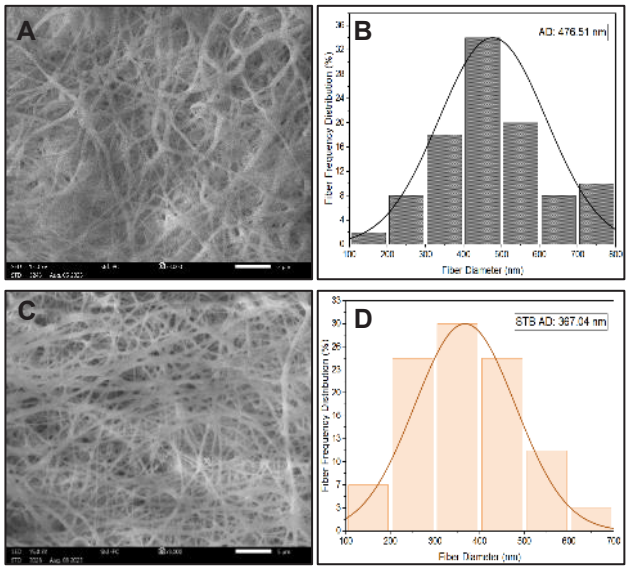

Fig 2. As-spun nanofibers electrospun from a 21.70 wt% solution at a spinning distance of 12.5 cm: (A) As-spun and (C) Stabilised nanofibers, with corresponding histograms of fiber diameter frequency distributions (B) and (D), respectively.

Following oxidative thermal stabilisation in air at 250°C, the nanofibers retained their continuous fibrous architecture without evidence of inter-fiber fusion or structural breakage, as demonstrated in Figure 2 (C). However, a marked reduction in average fiber diameter was observed, with the stabilised average diameter decreasing to 367.04 nm, as reflected in the fiber diameter distribution histogram in Figure 2 (D), where the distribution shifts notably toward smaller diameter values with the majority of fibers now concentrated in the 300-400 nm range.

The Energy-dispersive X-ray spectroscopy (EDX) spectra in Figure 3 confirm the presence of only three elements C, O, and Na across both the as spun and stabilised fibres, with no extraneous peaks detected, signifying chemical process integrity and absence of contamination.

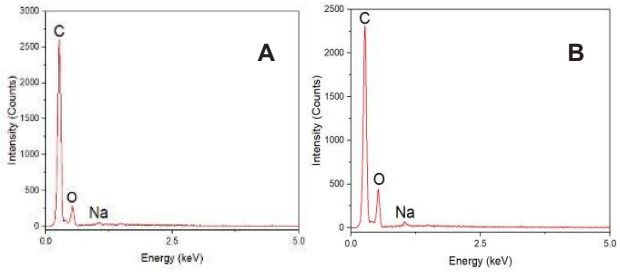

Fig 3. Elemental characterisation of LCNF through EDX: (A) as spun and (B) stabilised nanofibers.

The most significant change is the substantial increase in oxygen content from 22 at% in the as-spun fibers to 29 at% after oxidative thermal stabilisation, as shown in Table 2, accompanied by a corresponding decrease in carbon atomic percent from 77 at% to 70 at%, the concurrent reduction in carbon atomic percentage which is not attributable to carbon pyrolytic loss but could rather reflect a compositional dilution effect. The incorporation of oxygen atoms into the fibre matrix necessarily reduces the relative atomic fraction of carbon within the normalised compositional sum. This trend is entirely consistent with the expected chemistry of oxidative stabilisation.

Table 2: LCNF EDX Analysis (Atomic percentage, at%)

Element	As-spun (atom%)	Stabilised (atom%)	Change
C	77.48 ± 0.92	70.43 ± 0.89	−7.05 (−9.1%)
O	22.18 ± 1.34	29.06 ± 1.40	+6.88 (+31.0%)
Na	0.34 ± 0.08	0.51 ± 0.10	+0.17 (+50%)

3.2 Electrochemical performance of LCNF electrode

The electrochemical behaviour of the electrospun post-carbonisation carbon nanofiber (CNF) electrode was investigated by cyclic voltammetry (CV) in a three-electrode cell configuration comprising the CNF working electrode, a graphite plate counter electrode, and an Ag/AgCl (3.0 M KCl) reference electrode. Measurements

were performed in a 0.05 M vanadium solution prepared by dilution from a 1.6 M stock vanadium electrolyte in 4 M H_2SO_4 and 0.1 M H_3PO_4, over a potential window of -0.85 to 0.42 V vs. Ag/AgCl at scan rates ranging from 10 to 100 mV/s. At this vanadium concentration, the electrochemical response is predominantly influenced by the acidic supporting electrolyte. The CV characterisation therefore serves principally to probe the intrinsic surface electrochemistry, capacitive properties, and charge transfer characteristics of the CNF electrode material in a chemically representative environment, rather than to resolve discrete vanadium redox couples in isolation [11].

The voltammograms recorded across all scan rates, presented in Figure 4, exhibit a quasi-rectangular profile characteristic of a mixed capacitive-faradaic charge storage mechanism, as widely reported for carbonaceous electrode materials [12]. This profile deviates from both the ideal rectangle expected of a purely electrochemical double-layer capacitive (EDLC) electrode, where current is instantaneous and constant across the entire potential sweep, and the sharp, symmetric anodic-cathodic peak pairs associated with fully reversible faradaic systems [13, 14]. The observed behaviour thus reflects the concurrent operation of electrostatic double-layer charging at the carbon surface and broad, potential-distributed pseudocapacitive contributions from electroactive surface functional groups retained during the carbonisation process [12]. The rounded voltammetric corners, rather than the abrupt current transitions of an ideal capacitor, indicate finite ion diffusion and charge transfer kinetics within the porous nanofiber structure. The gradual current slope sustained across the potential sweep further evidences a distributed internal resistance arising from the heterogeneous pore structure of the CNF mat, where regions of varying fibre packing density and pore tortuosity contribute differentially to the aggregate electrochemical response [15].

In Figure 4, a systematic and progressive enlargement of the enclosed voltammetric area and peak current density is observed with increasing scan rate, with the current density increasing from approximately ±0.5 mA/g at 10 mV/s to ±2.0 mA/g at 100 mV/s. This proportional scaling of current with scan rate is consistent with a surface-confined charge storage process [12], in which dominant contributions arise from double-layer charging and pseudocapacitive interfacial reactions rather than from semi-infinite diffusion-controlled bulk processes. At lower scan rates (10-30 mV/s), the relatively symmetric and undistorted voltammetric profiles indicate that slow polarisation affords sufficient time for ions to penetrate the internal pore surfaces of the nanofiber network, with charge transfer proceeding at low overpotential demand.

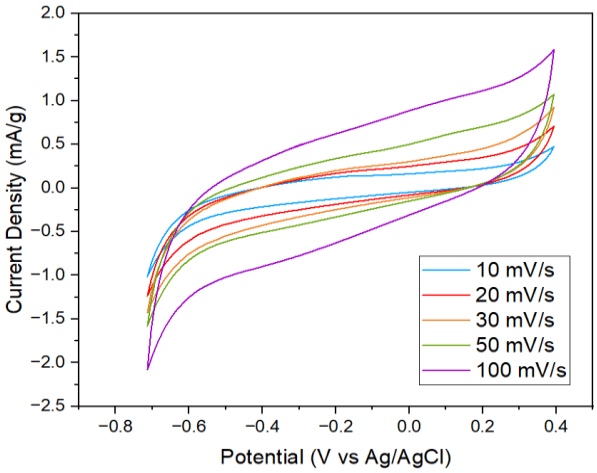

Fig 4. Cyclic voltammetry of LCNF (scan rate 10-100 mV/s)

This response is indicative of the good electronic conductivity characteristic of post-carbonisation CNF materials, in which thermal treatment promotes the development of a partially graphitic carbon microstructure that allows efficient electron transport through the fibre network. At higher scan rates (50-100 mV/s), progressive elongation and tilting of the voltammetric loop are observed, accompanied by growing asymmetry between the anodic and cathodic sweeps. This is consistent with the combined onset of ohmic polarisation and ion diffusion limitations within the tortuous pore channels of the nanofiber mat under faster polarisation, a behaviour well-documented for electrospun CNF systems [8].

Figure 5 extends the scan rate range from 100 to 500 mV/s, revealing important high-rate kinetic characteristics of the CNF electrode. The current density envelope increases noticeably, reaching approximately ±6 mA/g at 500 mV/s, demonstrating a sustained and proportional increase in current response with scan rate that is characteristic of a predominantly surface-confined charge storage process [12]. Critically, the quasi-rectangular profile is preserved across the entire extended scan rate range, with no collapse of the voltammetric envelope which indicate structural stability. This retention of coherent voltammetric morphology at high scan rates is a meaningful indicator of the electrode's rate capability, reflecting the rapid charge reproduction afforded by the interconnected conductive nanofiber network. At 500 mV/s, the voltammetric loop shows pronounced elongation and curvature relative to lower scan rates, with the anodic and cathodic current responses increasingly asymmetric features consistent with dominant ohmic polarisation and the transition toward diffusion-limited ion transport within the pore network at high-rate conditions.

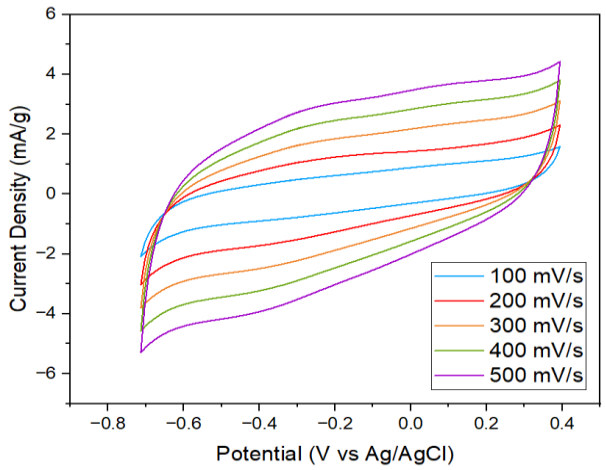

Fig 5. Cyclic voltammetry of LCNF (scan rate between 100-500 mV/s)

4 Conclusion

This study has demonstrated the feasibility of fabricating lignin-derived carbon nanofiber electrodes for vanadium redox flow battery applications via electrospinning of alkali lignin/PVP blends in DMF, followed by thermal stabilisation and carbonisation. The systematic investigation of electrospinning process parameters using a central composite design revealed that solution concentration is the dominant parameter governing fiber morphology and quality. Bead-free, interconnected nanofiber networks with high diameter uniformity were reliably achieved at polymer concentrations of 20 wt% and above, while lower concentrations produced defective beaded morphologies attributable to insufficient chain entanglement. Mean fiber diameters ranged from 163 nm to 476 nm depending on the processing conditions, with higher concentrations consistently yielding larger diameters due to the increased viscoelastic resistance of the spinning solution.

A 23% reduction in mean fiber diameter was observed upon stabilisation, consistent with literature reports for alkali lignin/PVP systems, and the carbonised mats retained their structural integrity through pyrolysis, confirming the effectiveness of the stabilisation step in preventing structural collapse. Electrochemical characterisation by cyclic voltammetry demonstrated that the LCNF electrode exhibits a quasi-rectangular voltammetric response across scan rates from 10 to 500 mV/s, indicative of a mixed double-layer capacitive and pseudocapacitive charge storage mechanism. The current density scaled proportionally with scan rate, increasing from ±0.5 mA/g at 10 mV/s to ±6 mA/g at 500 mV/s, confirming a predominantly surface-confined charge storage process and demonstrating the good rate capability of the material. The preservation of coherent voltammetric morphology at high scan rates further evidences the electrochemical stability and rapid charge propagation afforded by the interconnected conductive nanofiber network. Collectively, these findings confirm that alkali lignin is a viable bio-derived precursor for electrospun carbon nanofiber VRFB electrodes, offering a sustainable and potentially low-cost alternative to PAN-based materials. Future work will include FTIR, Raman spectroscopy, EIS, chronoamperometry, BET, XRD and TEM analyses, together with galvanostatic charge-discharge testing and long-term cycling stability studies, to establish the structure-performance relationship and practical durability of lignin-based carbon nanofiber electrodes for VRFBs.

This work is based on the research supported in part by the National Research Foundation of South Africa (TTK2204112994).

References

1. Vivo-Vilches JF, Celzard A, Fierro V, Devin-Ziegler I, Brosse N, Dufour A, et al. Lignin-based carbon nanofibers as electrodes for vanadium redox couples electrochemistry. Nanomaterials, 9:106, (2019). https://doi.org/10.3390/nano9010106.
2. He X, Li L, Yan S, Fu H, Zhong F, Cao J, et al. Advanced electrode enabled by lignin-derived carbon for high-performance vanadium redox flow battery. J Colloid Interface Sci, 653:1455–63, (2024). https://doi.org/10.1016/j.jcis.2023.10.005.
3. Maleki M, El-Nagar GA, Bernsmeier D, Schneider J, Roth C. Fabrication of an efficient vanadium redox flow battery electrode using a free-standing carbon-loaded electrospun nanofibrous composite. Sci Rep, 10:11153, (2020). https://doi.org/10.1038/s41598-020-67906-6.
4. Leba Akman A, Arslan MZ, Farsak M. The rise of vanadium redox flow batteries: A game-changer in energy storage. J Alloys Compd, 1038:182869, (2025). https://doi.org/10.1016/j.jallcom.2025.182869.

5. Lin CH, Zhuang Y De, Tsai DG, Wei HJ, Liu TY. Performance Enhancement of Vanadium Redox Flow Battery by Treated Carbon Felt Electrodes of Polyacrylonitrile using Atmospheric Pressure Plasma. Polymers (Basel) 12:1372, (2020). https://doi.org/10.3390/polym12061372.

6. Zhao Y, Li Y, Ihsan-Ul-haq M, Mubarak N, Xu M, Qin X, et al. Highly porous carbon nanofiber electrodes for vanadium redox flow batteries. Nanoscale, 14:5804–13, (2022). https://doi.org/10.1039/d1nr08376g.

7. Svinterikos E, Zuburtikudis I, Al-Marzouqi M. Electrospun Lignin-Derived Carbon Micro- and Nanofibers: A Review on Precursors, Properties, and Applications. ACS Sustain Chem Eng, 8:13868–93, (2020). https://doi.org/10.1021/acssuschemeng.0c03246.

8. Crespo Ribadeneyra M, Grogan L, Au H, Schlee P, Herou S, Neville T, et al. Lignin-derived electrospun freestanding carbons as alternative electrodes for redox flow batteries. Carbon N Y, 157:847–56, (2020). https://doi.org/10.1016/J.CARBON.2019.11.015.

9. Taş M, Elden G. A comprehensive review of carbon-based and metal-based electrocatalysts in the vanadium redox flow battery. Energy Storage, 4:e265, (2022). https://doi.org/10.1002/est2.265.

10. He X, He Z, Zou Q, Wu L. Carbon paper decorated with tin dioxide particle via in situ electrodeposition as bifunctional electrode for vanadium redox flow battery. Int J Energy Res, 44:2100–9, (2020). https://doi.org/10.1002/er.5068.

11. Parasuraman A, Lim TM, Menictas C, Skyllas-Kazacos M. Review of material research and development for vanadium redox flow battery applications. Electrochim Acta, 101:27–40, (2013). https://doi.org/10.1016/j.electacta.2012.09.067.

12. Simon P, Gogotsi Y. Materials for electrochemical capacitors. Nature Materials, 7:11 2008;7:845–54, (2008). https://doi.org/10.1038/nmat2297.

13. Bard AJ, Faulkner LR, Wiley J. Electrochemical Methods Fundamentals and Applications. Second. New York: John Wiley & Sons, Inc.; (2001).

14. Allagui A, Freeborn TJ, Elwakil AS, Maundy BJ. Reevaluation of Performance of Electric Double-layer Capacitors from Constant-current Charge/Discharge and Cyclic Voltammetry. Sci Rep 6:38568, (2016). https://doi.org/10.1038/srep38568.

15. Zhang L, Zhao XS. Carbon-based materials as supercapacitor electrodes. Chem Soc Rev 38:2520–31, (2009). https://doi.org/10.1039/b813846j.